Mineralogical Magazine, August 2013, Vol. 77(6), pp. 2841–2856

The dumortierite supergroup. II. Three new minerals from the Szklary pegmatite, SW Poland: Nioboholtite, $(Nb_{0.6}\square_{0.4})Al_6BSi_3O_{18}$, titanoholtite, $(Ti_{0.75}\square_{0.25})Al_6BSi_3O_{18}$, and szklaryite, $\square Al_6BAs_3^{3+}O_{15}$

A. Pieczka[1,*], R. J. Evans[2], E. S. Grew[3], L. A. Groat[2], C. Ma[4] and G. R. Rossman[4]

[1] Department of Mineralogy, Petrography and Geochemistry, AGH University of Science and Technology, Mickiewicza 30, Kraków, 30-059, Poland
[2] Department of Earth, Ocean and Atmospheric Sciences, University of British Columbia, 6339 Stores Road, Vancouver, British Columbia, V6T IZ4, Canada
[3] School of Earth and Climate Sciences, University of Maine, Bryand Global Science Center, Orono, Maine, 04469-5790, USA
[4] Division of Geological and Planetary Sciences, California Institute of Technology, MS 170-25, Pasadena, California, 91125-2500, USA

[*Received 26 December 2013; Accepted 11 July 2013; Associate Editor: A. Christy*]

ABSTRACT

Three new minerals in the dumortierite supergroup were discovered in the Szklary pegmatite, Lower Silesia, Poland. Nioboholtite, endmember $(Nb_{0.6}\square_{0.4})Al_6B_3Si_3O_{18}$, and titanoholtite, endmember $(Ti_{0.75}\square_{0.25})Al_6B_3Si_3O_{18}$, are new members of the holtite group, whereas szklaryite, endmember $\square Al_6BAs_3^{3+}O_{15}$, is the first representative of a potential new group. Nioboholtite occurs mostly as overgrowths not exceeding 10 μm in thickness on cores of holtite. Titanoholtite forms patches up to 10 μm across in the holtite cores and streaks up to 5 μm wide along boundaries between holtite cores and the nioboholtite rims. Szklaryite is found as a patch ~2 μm in size in As- and Sb- bearing dumortierite enclosed in quartz. Titanoholtite crystallized almost simultaneously with holtite and other Ta-dominant minerals such as tantalite-(Mn) and stibiotantalite and before nioboholtite, which crystallized simultaneously with stibiocolumbite during decreasing Ta activity in the pegmatite melt. Szklaryite crystallized after nioboholtite during the final stage of the Szklary pegmatite formation. Optical properties could be obtained only from nioboholtite, which is creamy-white to brownish yellow or grey-yellow in hand specimen, translucent, with a white streak, biaxial (−), $n_\alpha = 1.740-1.747$, $n_\beta \sim 1.76$, $n_\gamma \sim 1.76$, and $\Delta < 0.020$. Electron microprobe analyses of nioboholtite, titanoholtite and szklaryite give, respectively, in wt.%: P_2O_5 0.26, 0.01, 0.68; Nb_2O_5 5.21, 0.67, 0.17; Ta_2O_5 0.66, 1.18, 0.00; SiO_2 18.68, 21.92, 12.78; TiO_2 0.11, 4.00, 0.30; B_2O_3 4.91, 4.64, 5.44; Al_2O_3 49.74, 50.02, 50.74; As_2O_3 5.92, 2.26, 16.02; Sb_2O_3 10.81, 11.48, 10.31; FeO 0.51, 0.13, 0.19; H_2O (calc.) 0.05, −, −, Sum 96.86, 96.34, 97.07, corresponding on the basis of O = 18–As–Sb to $\{(Nb_{0.26}Ta_{0.02}\square_{0.18})(Al_{0.27}Fe_{0.05}Ti_{0.01})\square_{0.21}\}_{\Sigma 1.00}Al_6B_{0.92}\{Si_{2.03}P_{0.02}(Sb_{0.48}As_{0.39}Al_{0.07}\}_{\Sigma 3.00}(O_{17.09}OH_{0.04}\square_{0.87})_{\Sigma 18.00}$, $\{(Ti_{0.32}Nb_{0.03}Ta_{0.03}\square_{0.10})(Al_{0.35}Ti_{0.01}Fe_{0.01})\square_{0.15}\}_{\Sigma 1.00}Al_6B_{0.86}\{Si_{2.36}(Sb_{0.51}As_{0.14})\}_{\Sigma 3.01}(O_{17.35}\square_{0.65})_{\Sigma 18.00}$ and $\{\square_{0.53}(Al_{0.41}Ti_{0.02}Fe_{0.02})(Nb_{0.01}\square_{0.01})\}_{\Sigma 1.00}Al_6B_{1.01}\{(As_{1.07}Sb_{0.47}Al_{0.03})Si_{1.37}P_{0.06}\}_{\Sigma 3.00}(O_{16.46}\square_{1.54})_{\Sigma 18.00}$. Electron backscattered diffraction indicates that the three minerals are presumably isostructural with dumortierite, that is, orthorhombic symmetry, space group *Pnma*

* E-mail: pieczka@agh.edu.pl
DOI: 10.1180/minmag.2013.077.6.10

(no. 62), and unit-cell parameters close to $a = 4.7001$, $b = 11.828$, $c = 20.243$ Å, with $V = 1125.36$ Å^3 and $Z = 4$; micro-Raman spectroscopy provided further confirmation of the structural relationship for nioboholtite and titanoholtite. The calculated density is 3.72 g/cm^3 for nioboholtite, 3.66 g/cm^3 for titanoholtite and 3.71 g/cm^3 for szklaryite. The strongest lines in X-ray powder diffraction patterns calculated from the cell parameters of dumortierite of Moore and Araki (1978) and the empirical formulae of nioboholtite, titanoholtite and szklaryite are [*d*, Å, *I* (*hkl*)]: 10.2125, 67, 46, 19 (011); 5.9140, 40, 47, 57 (020); 5.8610, 66, 78, 100 (013); 3.4582, 63, 63, 60 (122); 3.4439, 36, 36, 34 (104); 3.2305, 100, 100, 95 (123); 3.0675, 53, 53, 50 (105); 2.9305, 65, 59, 51 (026); 2.8945, 64, 65, 59 (132), respectively. The three minerals have been approved by the IMA CNMNC (IMA 2012-068, 069, 070) and were named for their relationship to holtite and occurrence in the Szklary pegmatite, respectively.

Keywords: nioboholtite, titanoholtite, szklaryite, holtite group, dumortierite supergroup, new minerals, Szklary, Poland.

Introduction

Part 1 (Pieczka *et al*., 2013) reports a new nomenclature for minerals of the dumortierite supergroup, including background on the history and crystal structures of the three minerals presently constituting the supergroup: dumortierite, endmember $(Al)Al_6BSi_3O_{18}$, magnesiodumortierite, endmember $(Mg)Al_6BSi_3O_{17}(OH)$, and holtite, endmember $(Ta_{0.6}\square_{0.4})Al_6B_3Si_3O_{18}$ (Pieczka *et al.*, 2013). Here we describe three new minerals in the dumortierite supergroup from the Szklary pegmatite, Lower Silesia, Poland: nioboholtite, endmember $(Nb_{0.6}\square_{0.4})Al_6B_3Si_3O_{18}$, titanoholtite, endmember $(Ti_{0.75}\square_{0.25})Al_6B_3Si_3O_{18}$, and szklaryite, endmember $\square Al_6BAs_3^{3+}O_{15}$. The three minerals have been approved by the Commission on New Minerals, Nomenclature and Classification (CNMNC) of the International Mineralogical Association (IMA 2012-068, 069, and 070, respectively). Nioboholtite and titanoholtite are named for being the Nb-dominant and Ti-dominant analogues of holtite, whereas szklaryite is named for the type locality, Szklary, in Lower Silesia, Poland.

Type material of all three new minerals is preserved in the form of two polished 1-inch discs at the Mineralogical Museum of the University of Wrocław, Faculty of Earth Science and Environmental Management, Institute of Geological Sciences, 50-205 Wrocław, Cybulskiego 30, Poland, with the catalogue numbers MMWr IV7615 (nioboholtite, szklaryite) and MMWr IV7617 (titanoholtite). Nioboholtite and titanoholtite cotype specimens are preserved at the above-mentioned museum with the catalogue numbers MMWr IV7616 – MMWr IV7619, and MMWr IV7620 – MMWr IV7621, respectively. Cotype material of nioboholtite and titanoholtite has also been deposited in the National Museum of Natural History (Smithsonian Institution) as catalogue numbers NMNH 175986, NMNH 175987 and NMNH 175988 (each disc contains both minerals).

Parent pegmatite and paragenesis

Nioboholtite, titanoholtite and szklaryite (originally described as holtite and dumortierite by Pieczka *et al*., 2011) occur with aggregates of holtite in a single dyke of a complex zoned granitic pegmatite in the Szklary serpentinite massif, ~60 km south of Wrocław, Lower Silesia, SW Poland (latitude 50°39.068′; longitude 16°49.932′), in the southern part of the Mississippian Niemcza shear zone that extends along the eastern edge of the Sowie Mountains block in the northeastern part of the Bohemian Massif.

The dyke, ~1 m thick, is exposed in a 4 m × 1 m area in one of the open pits of the abandoned Marta mine of silicate nickel ores in the northern part of Szklana Hill at Szklary. The border zone of the dyke is composed dominantly of quartz, albite, golden-brown biotite, black tourmaline, subordinate grass-green clinochlore and very local cordierite. Albite is gradually replaced inward by microcline-perthite, and there is a gradation into the coarsely crystalline internal zone with accumulations of muscovite and black tourmaline, but with the absence of biotite. Tourmaline is commonly represented by dark, Fe^{3+}-bearing, Li-free intermediate members of the schorl–dravite series (Pieczka and Kraczka, 1996), or, less commonly, by blue dravite representing a transitional member among the dravite, schorl and olenite endmembers (Pieczka, 2007).

The pegmatite-forming magma could be derived from anatexis of the sedimentary complex of the nearby Sowie Mountains block; these processes generated intrusions of granitic magma during uplift at ~374–380 Ma (van Breemen *et al.*, 1988; Timmermann *et al.*, 2000). The Szklary dyke (~382 Ma; Pieczka, unpublished data) is inferred to be such an anatectic melt emplaced during a HT–MP event into an adjacent part of the Sudetic ophiolite currently known as the Szklary massif. A talc + chlorite + vermiculite contact zone between the pegmatite on one side and serpentinite and amphibolite on the other (Pieczka, 2000) is interpreted to have formed by reaction between melt and country rocks, and to have retrogressed subsequently. The reaction resulted in the loss of SiO_2 and gain of Al_2O_3 by the melt, thereby favouring the direct crystallization of Al-bearing minerals, including members of the dumortierite supergroup.

Holtite, nioboholtite, titanoholtite, szklaryite, As- and Sb-bearing dumortierite and stibiocolumbite (which in places encloses holtite fibres), form small aggregates up to a few millimeters across, occurring in the microcline-quartz-muscovite matrix of the internal zone. Nioboholtite commonly forms a rim overgrown around a core of holtite in zoned crystals, which occur in the internal zone of the pegmatite (Fig. 1*a*–*f*). The rims are mostly ~5 μm thick and do not exceed 10 μm. In exceptional cases, nioboholtite forms a core of zoned crystals, in which case it is overgrown by As- and Sb-bearing dumortierite. Titanoholtite occurs in patches up to 10 μm across and streaks up to 5 μm wide, located in the cores of holtite or along the boundaries between the holtite cores and nioboholtite rims. Szklaryite is found as a single patch ~2 μm in size in As- and Sb-bearing dumortierite up to 15 μm across enclosed in quartz (Fig. 1*g*,*h*). In the back-scattered electron (BSE) micrograph of Fig. 1*h*, the lightest patches are szklaryite, and darker areas represent As- and Sb-bearing dumortierite.

Associated minerals include spessartine, chrysoberyl, zircon, monazite-(Ce), cheralite, xenotime-(Y), Mn-rich fluor-, hydroxyl- and chlorapatite, beusite, columbite-(Fe), columbite-(Mn), tantalite-(Mn), stibiocolumbite, stibiotantalite, fersmite, pyrochlore-supergroup minerals represented by various members of the pyrochlore, microlite and betafite groups, Mn oxides such as hollandite, romanèchite and possible coronadite, ranciéite and ernienickelite, uraninite, thorutite, native Sb, As, Bi and Au, stibarsen and paradocrasite, pollucite, natrophyllite, purpurite, alluaudite, gorceixite, plumbogummite, phosphohedyphane, mitridatite, saponite, nontronite, and also a few unnamed minerals. Stibiocolumbite in places encloses zoned fibres composed of the holtite-group minerals; in general, many of the minerals occur only as tiny inclusions.

Crystallization of the dumortierite-supergroup minerals in the pegmatite began when the availability of Ta in the pegmatite-forming melt was greatest, so that holtite with typical Ta-dominant compositions and the highest Ta/(Ta+Nb) ratios crystallized first (Pieczka, 2010; Pieczka *et al.*, 2011). Titanoholtite crystallized under decreasing Ta activity almost simultaneously with holtite and other Ta-dominant minerals such as tantalite-(Mn) and stibiotantalite, followed by columbite-(Mn) and stibiocolumbite. Patches of titanoholtite within the holtite cores probably resulted from a localized increase in availability of Ti relative to Ta and Nb. Nioboholtite crystallized after holtite and titanoholtite, simultaneously with stibiocolumbite, under further decreasing Ta activity, when holtite, titanoholtite and stibiocolumbite became progressively richer in Nb, so that in the outermost zone of holtite crystals Nb predominates over Ta, forming nioboholtite. Preservation of the fine zoning in the crystals is most likely due to the relatively low diffusion coefficients for quadrivalent and pentavalent cations (Brady and Cherniak, 2010). Szklaryite crystallized after nioboholtite, but before As- and Sb-enriched dumortierite, under unusually high As and Sb activities, extremely low S activities, and low Ta, Nb and Ti activities, all the latter elements having been consumed during crystallization of the Nb-Ta oxides and the minerals of the holtite group.

Physical properties

Optical properties could be obtained only from nioboholtite, measurements of titanoholtite and szklaryite were not possible due to their grains being too small to extract for study. Nioboholtite is creamy-white to yellow, brownish yellow or yellowish-grey in hand specimen, translucent, and has a white streak. The mineral is biaxial (–) with $n_\alpha = 1.740–1.747$, $n_\beta \sim 1.76$, $n_\gamma \sim 1.76$, and $\delta < 0.020$. The calculated density is 3.72 g/cm^3 for nioboholtite, 3.66 g/cm^3 for titanoholtite and 3.71 g/cm^3 for szklaryite.

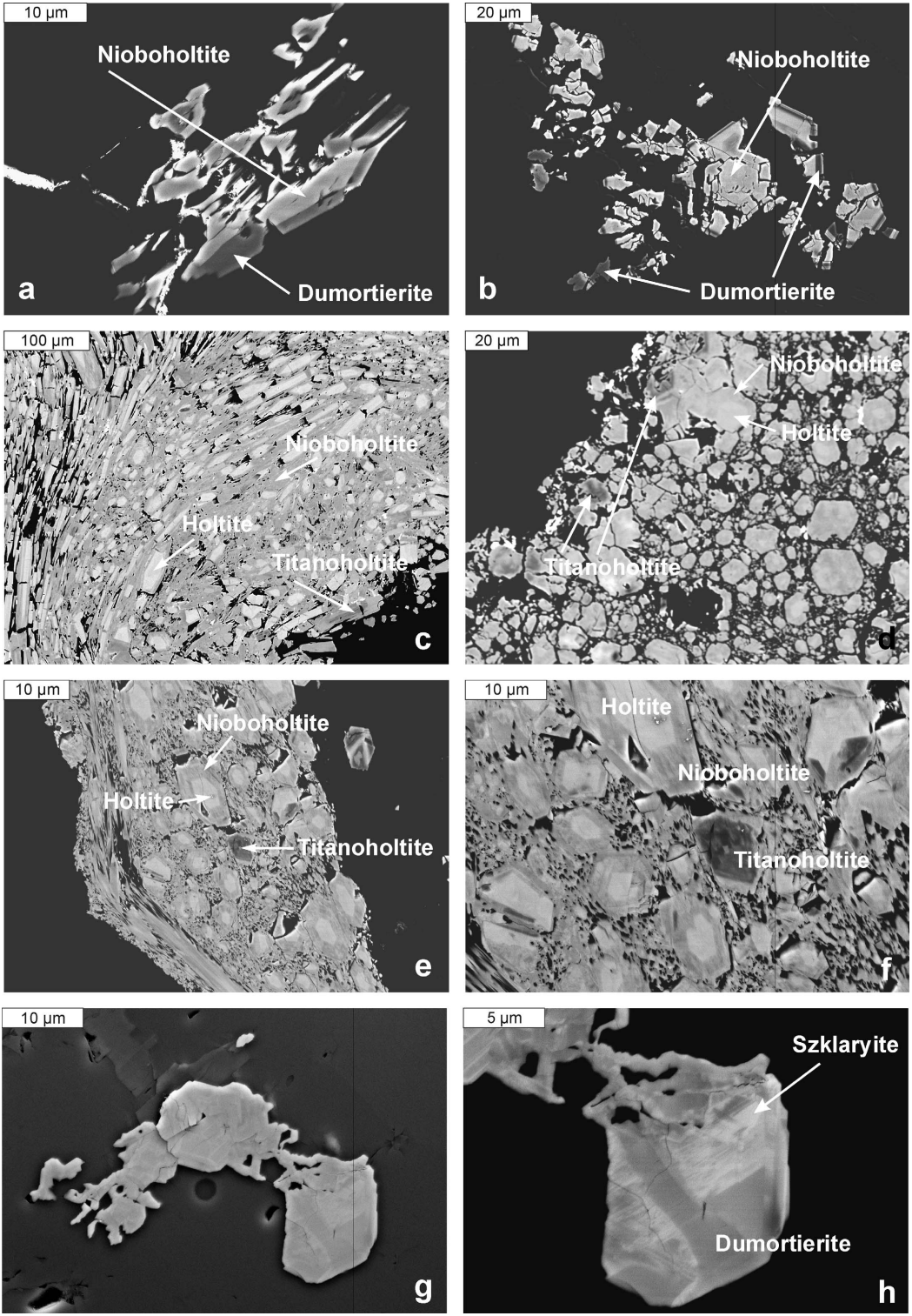
10 μm
Nioboholtite
Dumortierite
a
20 μm
Nioboholtite
Dumortierite
b
100 μm
Nioboholtite
Holtite
Titanoholtite
c
20 μm
Nioboholtite
Holtite
Titanoholtite
d
10 μm
Nioboholtite
Holtite
Titanoholtite
e
10 μm
Holtite
Nioboholtite
Titanoholtite
f
10 μm
g
5 μm
Szklaryite
Dumortierite
h

Crystallography

Single-crystal X-ray diffraction studies could not be carried out because of the small size of the minerals and their intergrowth with other dumortierite-supergroup minerals. Instead, the three minerals were characterized by electron-back-scattered diffraction (EBSD). Single-crystal electron back-scatter diffraction analyses at a submicrometer scale were performed at Caltech using an HKL EBSD system on a ZEISS 1550VP scanning electron microscope, operated at 20 kV and 6 nA in focused beam mode with a 70° tilted stage and in a variable pressure mode (25 Pa) (Ma and Rossman, 2008, 2009). The structure was determined and cell constants were obtained by matching the experimental EBSD pattern with the dumortierite and holtite structures (Moore and Araki, 1978; Alexander *et al*., 1986; Hoskins *et al*., 1989). In the case of each of the new minerals, EBSD patterns (Fig. 2) were indexed by the dumortierite-holtite structure to give a best fit based on unit-cell data for dumortierite from Moore and Araki (1978), with mean angular deviations of 0.49° for the nioboholtite, 0.45° for titanoholtite and 0.47° for szklaryite. These matches confirmed that nioboholtite, titanoholtite and szklaryite have similar unit-cell parameters to, and are presumably isostructural with, dumortierite and holtite, and have orthorhombic symmetry, space group *Pnma* (no. 62), and unit-cell parameters close to those obtained by Moore and Araki (1978) for dumortierite: a = 4.7001 Å, b = 11.828 Å, c = 20.243 Å, with V = 1125.36 Å^3 and Z = 4. X-ray powder diffraction data (Cu$K\alpha_1$, Bragg-Brentano geometry) were calculated from the cell parameters of Moore and Araki (1978) on the basis of the mean empirical formula of each new mineral using *Powder Cell* version 2.4 (Table 1).

Raman spectroscopy

MicroRaman spectroscopy was performed at Caltech using a Renishaw M-1000 microRaman system with a depolarized 514.5 nm laser and a 100× objective with ~5.5 mW power at the sample in a roughly 1 μm diameter area. Attempts to obtain usable spectra from szklaryite were not successful, and many of the patterns of nioboholtite and titanoholtite had significant contamination from surrounding material. One of the better patterns for nioboholtite (Fig. 3*a*) shows the general features observed in a dumortierite standard from Dehesa, California, but shifted somewhat in position and intensity ratios. Additional weak features from quartz are also visible. The pattern can be taken as corroboration that nioboholtite is closely related to durmortierite. The titanoholtite gave a lower signal to background ratio than the dumortiertite standard (Fig. 3*b*). The spectrum showed contamination from the epoxy used to mount the sample, and due to the small size of the domain, it may be contaminated from the underlying or adjacent material. The more prominent Raman bands of titanoholtite are at 211, 286, 362, 407, 466, 507, 561, 624, 885, 935 and 1055 cm^{-1}. Although the intensities of the features in the titanoholtite spectrum are different from those of the dumortierite spectrum, their number and positions correspond to features in the dumortierite spectrum (Fig. 3*b*), thereby providing some corroboration of the structural relationship. Raman spectra obtained from the 3200–3600 cm^{-1} OH region for titanoholtite did not show any features. Likewise, the dumortierite Raman spectrum was also devoid of features in that region, even though the transmission infrared spectrum of the Dehesa dumortierite shows OH bands (Ma *et al*., 2002; Fuchs *et al*., 2005).

Chemical composition

Methods

Electron-microprobe analysis of the holotype specimens of nioboholtite, titanoholtite and szklaryite was carried out at the California Institute of Technology in the wavelength dispersive mode (WDS), using a Jeol JXA-8200

FIG. 1 (*facing page*). Backscattered electron micrographs of nioboholtite, titanoholtite and szklaryite from the Szklary pegmatite, Poland: (*a*) nioboholtite overgrown by As- and Sb-bearing dumortierite (MMWr IV7615 specimen); (*b*) nioboholtite overgrown by As- and Sb-bearing dumortierite (MMWr IV7615 specimen); (*c*) crystals showing light holtite cores and darker nioboholtite rims; the darkest streaks are titanoholtite (MMWr IV7616 specimen); (*d*) crystal of holtite overgrown with nioboholtite, containing irregular patches of titanoholtite (MMWr IV7617 specimen); (*e*) titanoholtite from the holotype specimen, enlarged in (*f*) (MMWr IV7617 specimen); (*g*) inclusions of As- and Sb-bearing dumortierite with szklaryite in quartz (dark) (MMWr IV7615 specimen); (*h*) enlargement of part *g*. showing szklaryite inclusions (the lightest portions) in As- and Sb-bearing dumortierite.

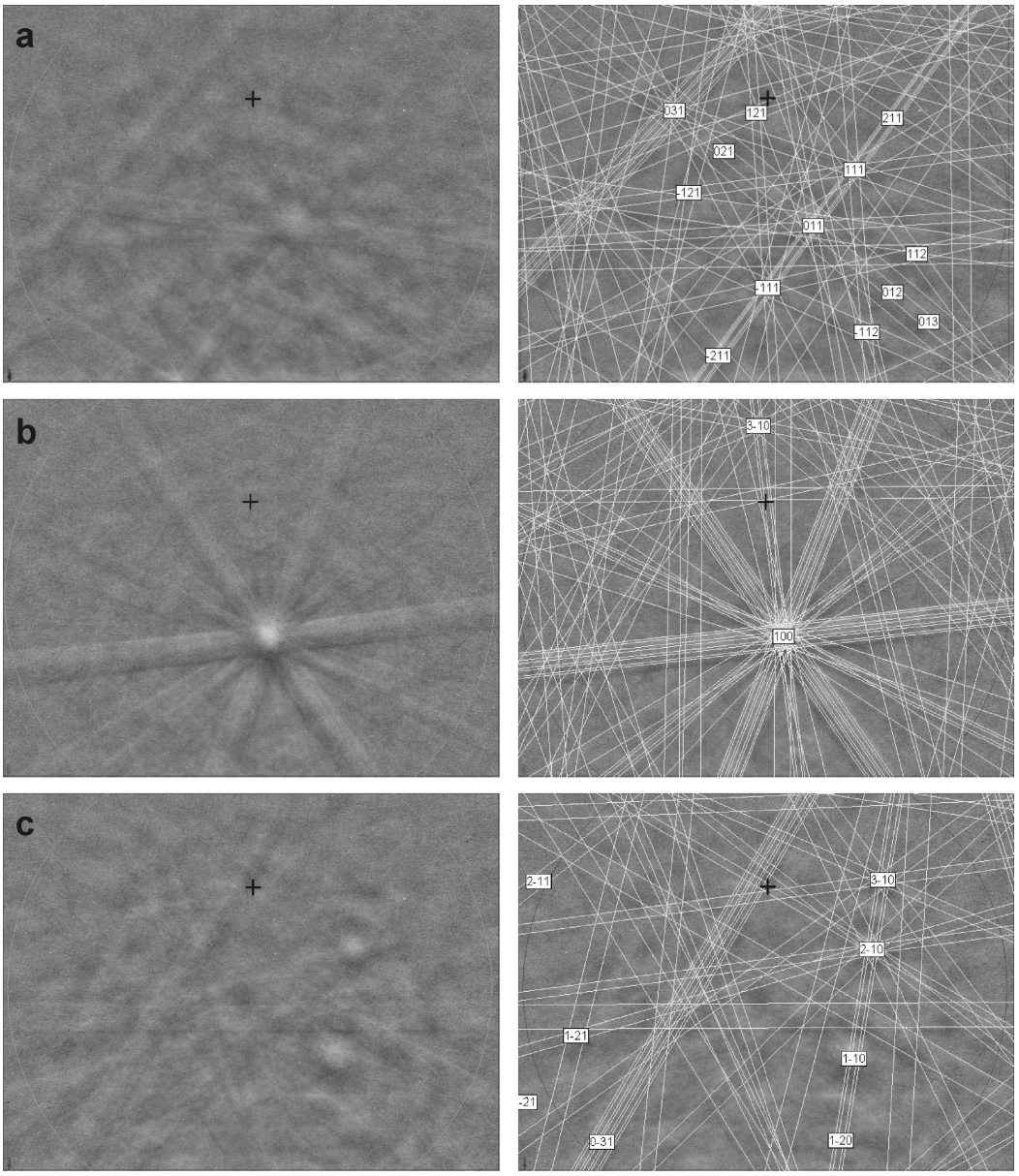

FIG. 2. EBSD patterns (left) and the patterns indexed with dumortierite, space group *Pnma* (Moore and Araki, 1978) (right). (*a*) Nioboholtite, (*b*) titanoholtite, (*c*) szklaryite.

instrument, an accelerating voltage of 10 kV, a beam current of 10 nA, and a beam diameter of 0.12 μm. In one set of analyses, B and O contents were assumed to be stoichiometric, and the following standards and X-ray analytical lines were used: apatite – P($K\alpha$), NbO – Nb($L\alpha$), Ta metal – Ta($M\alpha$), kyanite – Si($K\alpha$) and Al($K\alpha$), TiO_2 – Ti($K\alpha$), GaAs – As($K\alpha$), Sb metal – Sb($L\alpha$), and fayalite – Fe($K\alpha$). In a second set, B and O contents were also measured with danburite and kyanite as standards for B($K\alpha$) and O($K\alpha$), respectively, using LDEB and LDE1 analysing

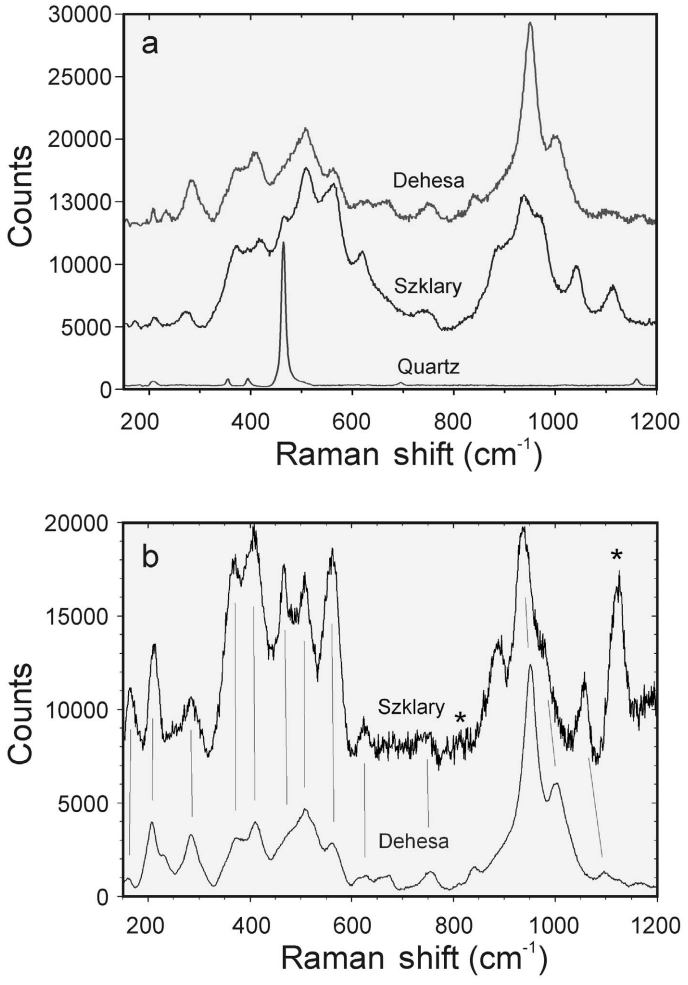

FIG. 3. (*a*) Raman spectrum of nioboholtite (sample MMWr IV7615) compared to the spectrum of dumortierite from Dehesa, California. (*b*) Raman spectrum of titanoholtite (sample MMWr IV7617; the grain identified as titanoholtite in Figs 1*e* and *f*) compared to the spectrum of a dumortierite standard from Dehesa, California. Bands marked with an asterisk and the high background at high wavenumbers at the far right side of the diagram are due to the epoxy used to mount the sample. Dumortierite was oriented such that the laser beam was normal to the {010} cleavage. For titanoholtite the laser was approximately normal to $(62\bar{1})$. The vertical lines indicate possible correlations between bands in dumortierite and titanoholtite.

crystals at 10 kV and 10 nA. Analyses of cotype specimens of nioboholtite and titanoholtite were carried out at the Inter-Institute Analytical Complex for Minerals and Synthetic Substances of University of Warsaw using a Cameca SX-100 electron microprobe operating in WDS mode with an accelerating voltage of 15 kV, a beam current of 20 nA, peak count-time of 20 s, background time of 10 s, a beam diameter of 1–2 μm. The following standards and analytical lines were used: apatite – P($K\alpha$), Nb metal – Nb($L\alpha$), Ta metal – Ta($M\alpha$), diopside – Si($K\alpha$), rutile – Ti($K\alpha$), orthoclase – Al($K\alpha$), GaAs – As($L\alpha$), InSb – Sb($L\beta$), and hematite – Fe($K\alpha$). Magnesium, Mn and Bi were below detection. Data were reduced with the 'PAP' procedure (Pouchou and Pichoir, 1985) in both laboratories.

Formulae were calculated by iteration on the basis of $[18 - (As^{3+} + Sb^{3+})]$ oxygen atoms per formula unit (a.p.f.u.), using the procedure

TABLE 1. Calculated powder X-ray data for nioboholite, titanoholtite and szklaryite (I_{rel} > 1).

h	*k*	*l*	*d* (Å)	Nioboholtite I_{rel}	Titanoholtite I_{rel}	Szklaryite I_{rel}
0	1	1	10.2125	67	46	19
0	0	2	10.1215	19	11	3
0	2	0	5.9140	40	47	57
0	1	3	5.8610	66	78	100
0	2	2	5.1062	12	13	
0	0	4	5.0608	8	9	
1	1	1	4.2696	10	12	6
1	0	2	4.2629	5	6	3
1	1	2	4.0104	2	3	
0	3	1	3.8700	11	10	2
0	2	4	3.8451	12	10	3
0	1	5	3.8304	11	9	2
1	2	1	3.6203	22	20	27
1	2	2	3.4582	63	63	60
1	0	4	3.4439	36	36	34
0	3	3	3.4042	5	5	
0	0	6	3.3738	2	2	
1	1	4	3.3066	24	24	23
1	2	3	3.2305	100	100	95
1	0	5	3.0675	53	53	50
1	3	1	2.9876	9	9	8
1	2	4	2.9761	5	5	5
1	1	5	2.9693	6	6	6
0	4	0	2.9570	28	25	22
0	2	6	2.9305	65	59	51
1	3	2	2.8945	64	65	59
0	4	2	2.8384	3	2	
0	3	5	2.8246	8	6	3
0	1	7	2.8091	3	2	
1	3	3	2.7570	3	2	3
1	2	5	2.7230	9	9	7
1	1	6	2.6701	24	26	20
0	4	4	2.5531	25	28	30
0	0	8	2.5304	11	12	14
1	4	1	2.4840	13	14	9
1	0	7	2.4630	17	18	15
1	4	2	2.4297	4	5	3
1	3	5	2.4210	8	9	5
1	1	7	2.4113	6	7	4
2	0	0	2.3501	8	8	7
0	5	1	2.3496	9	7	6
1	4	3	2.3466	25	25	23
2	0	1	2.3344	8	9	14
0	3	7	2.3319	7	5	4
0	2	8	2.3264	7	5	4
2	1	0	2.3050			2
1	4	4	2.2435	15	15	15
1	0	8	2.2280	9	9	8
0	4	6	2.2238			1
1	1	8	2.1895	8	8	8
2	2	0	2.1839	6	7	6
2	1	3	2.1812	13	15	12

Table 1 (*contd*.)

h	*k*	*l*	*d* (Å)	Nioboholtite I_{rel}	Titanoholtite I_{rel}	Szklaryite I_{rel}
2	2	2	2.1348	2	2	2
1	4	5	2.1289	12	12	13
1	5	1	2.1016	25	28	19
2	1	4	2.0977	2	2	
1	3	7	2.0889	22	25	17
1	2	8	2.0850	26	29	20
2	2	3	2.0778	3	2	
1	5	2	2.0685	4	4	3
2	0	5	2.0325	3	2	
2	3	0	2.0187	5	5	2
1	5	3	2.0165	2	2	2
2	3	1	2.0087	3	3	2
2	2	4	2.0052	2	2	
2	1	5	2.0031	4	5	3
2	3	2	1.9797	8	7	4
1	5	4	1.9499		2	
2	3	3	1.9340	3	3	
2	2	5	1.9221	4	5	
1	2	9	1.9191		2	
2	1	6	1.9032	4	4	
2	3	4	1.8750	13	12	6
1	1	10	1.8366	10	11	7
2	4	1	1.8322			3
2	0	7	1.8238	15	14	9
1	6	1	1.8106	7	2	
1	5	6	1.7908	5	9	5
1	6	2	1.7893	4	4	4
1	4	8	1.7794	22	4	4
2	4	3	1.7750	4	22	13
1	2	10	1.7736	9	4	4
1	6	3	1.7553	11	9	9
2	2	7	1.7428	9	12	17
2	3	6	1.7323	7	10	13
2	4	4	1.7291	2	8	7
2	0	8	1.7220	2	2	2
1	6	4	1.7109	3	2	2
1	5	7	1.7061	2	3	3
0	6	6	1.7021	2		

explained by Pieczka *et al*. (2013). We have assumed that Fe is entirely Fe^{2+} because Fe^{3+} contents are minor in associated Nb-Ta oxides (Pieczka, 2010; Pieczka *et al*., 2011). Grain size precluded direct measurement of H_2O content, and consequently, OH = 0, unless Fe^{2+} > Ti, which implies incorporation of the $Fe^{2+}Al_6BSi_3O_{17}OH$ endmember, i.e. OH = Fe^{2+} – Ti.

Many of the totals for the analyses performed at the California Institute of Technology and at the University of Warsaw range from 96 to 99 wt.%; holtite analysed at the University of British Columbia also gave low totals (Groat *et al*., 2009). Possible explanations for the low totals are:

infiltration of epoxy between the very fine fibres characteristic of the analysed dumortierite-supergroup minerals, creating a situation analogous to epoxy soaking very finely porous materials (Sorbier *et al*., 2004; Grew *et al*., 2008), in which analytical totals decreased because the target material was diluted by epoxy,

differences in chemical composition or crystal structure between the analysed material and standards (matrix effects),

the presence of H_2O molecules lodged in channels centred on the A11 position when the As sites are occupied and the Si sites are vacant, a situation that could arise most probably in szklaryite. The distances between the As sites across the channels range from 5.7 to 5.9 Å, i.e. the channels are roughly circular in section, and the distances exceed the channel diameter in beryl (5.1 Å), i.e. large enough to accommodate water molecules.

Results

For each of the three new minerals, Tables 2–4 give WDS spot analyses collected at Caltech, with direct determination of B, together with averages and standard deviations of the analysed components, as well as analyses obtained independently at Warsaw. Table 5 presents compositions of the co-type material. Compositional features shared by all three minerals include the presence of minor P and Fe and Mg below detection. Direct analyses of boron confirm the presence of B at close to stoichiometric amounts in szklaryite (1.00–1.03 B p.f.u.), and at amounts somewhat below stoichiometry in nioboholtite and titanoholtite (0.80–0.99 B p.f.u.). Nioboholtite and titanoholtite have Sb > As and Si > (Sb + As), whereas szklaryite has As > Sb and (As + Sb) > Si

TABLE 2. Representative compositions of szklaryite.

	#25[1]	#26[1]	#27[1]	av.[1]	sd[1]	Sz5a2[2]
Wt.%						
P_2O_5	0.48	0.60	0.78	0.62	0.15	0.99
Nb_2O_5	0.16	0.23	0.29	0.22	0.06	0.00
SiO_2	12.34	12.84	12.94	12.71	0.32	12.90
TiO_2	0.27	0.27	0.23	0.26	0.02	0.27
B_2O_3	5.34	5.47	5.51	5.44	0.08	5.49
Al_2O_3	50.66	50.71	50.86	50.74	0.11	51.88
As_2O_3	16.89	16.64	15.66	16.39	0.65	16.81
Sb_2O_3	10.87	10.47	10.14	10.49	0.36	10.23
FeO	0.26	0.14	0.15	0.18	0.06	0.20
$H_2O_{(calc.)}$	0.00	0.00	0.00	0.00	0.00	0.00
Total	97.27	97.37	96.57	97.07	0.44	98.76
Contents of ions on the basis of (O,OH) = 18–As–Sb p.f.u.						
P^{5+}	0.044	0.054	0.071	0.056	0.014	0.088
Nb^{5+}	0.008	0.011	0.014	0.011	0.003	0.000
Si^{4+}	1.332	1.379	1.397	1.369	0.033	1.362
Ti^{4+}	0.022	0.022	0.019	0.021	0.002	0.022
B^{3+}	0.996	1.015	1.026	1.012	0.015	1.000
Al^{3+}	6.444	6.419	6.471	6.444	0.010	6.457
As^{3+}	1.107	1.085	1.027	1.073	0.042	1.078
Sb^{3+}	0.484	0.464	0.452	0.467	0.016	0.446
Fe^{2+}	0.023	0.013	0.014	0.017	0.006	0.018
O^{2-}	16.407	16.451	16.522	16.460	0.058	16.476
$OH^-_{(calc.)}$	0.002	0.000	0.000	0.000	0.000	0.000

[1] analysis with direct WDS determination of B_2O_3, performed at Caltech (USA); [2] analysis with B_2O_3 calculated on the basis of stoichiometry, performed at University of Warsaw (Poland); Ta is below detection; av. – average; sd – standard deviation.

Szklaryite chemical formulae:

#25: $\{\square_{0.53}(Al_{0.41}Ti_{0.02}Fe_{0.02})(Nb_{0.01}\square_{0.01})\}_{\Sigma 1.00}Al_6B_{1.00}\{(As_{1.11}Sb_{0.48}Al_{0.03})Si_{1.33}P_{0.04}\}_{\Sigma 3.00}(O_{16.41}\square_{1.59})_{\Sigma 18.00}$

#26: $\{\square_{0.54}(Al_{0.40}Fe_{0.01}Ti_{0.01})(Nb_{0.01}Ti_{0.01}\square_{0.01})\}_{\Sigma 1.00}Al_6B_{1.01}\{(As_{1.00}Sb_{0.46}Al_{0.02})Si_{1.38}P_{0.05}\}_{\Sigma 3.00}(O_{16.45}\square_{1.55})_{\Sigma 18.00}$

#27: $\{\square_{0.53}(Al_{0.42}Fe_{0.01}Ti_{0.01})(Nb_{0.01}Ti_{0.01}\square_{0.01})\}_{\Sigma 1.00}Al_6B_{1.03}\{(As_{1.03}Sb_{0.45}Al_{0.05})Si_{1.40}P_{0.07}\}_{\Sigma 3.00}(O_{16.52}\square_{1.48})_{\Sigma 18.00}$

Average[1]: $\mathbf{\{\square_{0.53}(Al_{0.41}Ti_{0.02}Fe_{0.02})(Nb_{0.01}\square_{0.01})\}_{\Sigma 1.00}Al_6B_{1.01}\{(As_{1.07}Sb_{0.47}Al_{0.03})Si_{1.37}P_{0.06}\}_{\Sigma 3.00}(O_{16.46}\square_{1.54})_{\Sigma 18.00}}$

5a2[2]: $\{\square_{0.53}(Al_{0.43}Ti_{0.02}Fe_{0.02})\}_{\Sigma 1.00}Al_6B\{(As_{1.08}Sb_{0.45}Al_{0.03})Si_{1.36}P_{0.09}\}_{\Sigma 3.00}(O_{16.48}\square_{1.52})_{\Sigma 18.00}$

TABLE 3. Representative compositions of nioboholtite.

	#39[1]	#40[1]	#41[1]	#42[1]	av.[1]	sd[1]	5c10[2]
Wt.%							
P_2O_5	0.18	0.25	0.27	0.34	0.26	0.07	0.31
Nb_2O_5	5.19	5.22	5.01	5.42	5.21	0.16	5.05
Ta_2O_5	0.65	0.50	0.81	0.68	0.66	0.13	0.70
SiO_2	18.80	18.53	18.76	18.63	18.68	0.13	17.56
TiO_2	0.13	0.08	0.08	0.13	0.11	0.03	0.12
B_2O_3	4.83	5.12	5.28	4.41	4.91	0.38	5.35
Al_2O_3	49.90	49.88	49.67	49.50	49.74	0.19	49.59
As_2O_3	6.26	6.10	5.68	5.65	5.92	0.30	6.78
Sb_2O_3	11.00	10.82	10.61	10.81	10.81	0.16	11.58
FeO	0.63	0.45	0.42	0.53	0.51	0.09	0.37
$H_2O_{(calc.)}$	0.06	0.05	0.04	0.05	0.05	0.01	0.03
Total	97.65	97.00	96.64	96.17	96.86	0.62	97.46
Contents of ions on the basis of (O,OH) = 18–As–Sb p.f.u.							
P^{5+}	0.017	0.023	0.025	0.032	0.024	0.006	0.028
Nb^{5+}	0.253	0.255	0.245	0.269	0.256	0.010	0.247
Ta^{5+}	0.019	0.015	0.024	0.020	0.019	0.004	0.021
Si^{4+}	2.029	2.005	2.035	2.044	2.028	0.017	1.900
Ti^{4+}	0.011	0.007	0.007	0.011	0.009	0.002	0.009
B^{3+}	0.900	0.956	0.988	0.835	0.920	0.067	1.000
Al^{3+}	6.345	6.331	6.349	6.401	6.364	0.028	6.325
As^{3+}	0.410	0.401	0.374	0.377	0.390	0.018	0.446
Sb^{3+}	0.490	0.483	0.475	0.489	0.484	0.007	0.517
Fe^{2+}	0.057	0.041	0.039	0.048	0.046	0.008	0.034
O^{2-}	17.054	17.082	17.120	17.097	17.088	0.028	17.013
$OH^-_{(calc.)}$	0.046	0.034	0.032	0.037	0.037	0.006	0.024

[1] analysis with direct WDS determination of B_2O_3, performed at Caltech (U.S.A.); [2] analysis with B_2O_3 calculated on the basis of stoichiometry, performed at University of Warsaw (Poland); av. – average; sd – standard deviation.

Nioboholtite chemical formulae:

#39: $\{(Nb_{0.25}Ta_{0.02}\square_{0.14})(Al_{0.29}Fe_{0.06}Ti_{0.01})\square_{0.23}\}_{\Sigma 1.00}Al_6B_{0.90}\{Si_{2.03}P_{0.02}(Sb_{0.49}As_{0.41}Al_{0.05})\}_{\Sigma 3.00}(O_{17.05}OH_{0.05}\square_{0.90})_{\Sigma 18.00}$

#40: $\{(Nb_{0.26}Ta_{0.01}\square_{0.16})(Al_{0.27}Fe_{0.04}Ti_{0.01})\square_{0.25}\}_{\Sigma 1.00}Al_6B_{0.96}\{Si_{2.01}P_{0.02}(Sb_{0.48}As_{0.40}Al_{0.09})\}_{\Sigma 3.00}(O_{17.08}OH_{0.03}\square_{0.88})_{\Sigma 18.00}$

#41: $\{(Nb_{0.25}Ta_{0.02}\square_{0.17})(Al_{0.26}Fe_{0.04}Ti_{0.01})\square_{0.26}\}_{\Sigma 1.00}Al_6B_{0.99}\{Si_{2.03}P_{0.03}(Sb_{0.48}As_{0.37}Al_{0.09})\}_{\Sigma 3.00}(O_{17.12}OH_{0.03}\square_{0.85})_{\Sigma 18.00}$

#42: $\{(Nb_{0.27}Ta_{0.02}\square_{0.13})(Al_{0.34}Fe_{0.05}Ti_{0.01})\square_{0.18}\}_{\Sigma 1.00}Al_6B_{0.84}\{Si_{2.04}P_{0.03}(Sb_{0.49}As_{0.38}Al_{0.06})\}_{\Sigma 3.00}(O_{17.10}OH_{0.04}\square_{0.86})_{\Sigma 18.00}$

Average[1]: $\{(Nb_{0.26}Ta_{0.02}\square_{0.18})(Al_{0.27}Fe_{0.05}Ti_{0.01})\square_{0.21}\}_{\Sigma 1.00}Al_6B_{0.92}\{Si_{2.03}P_{0.02}(Sb_{0.48}As_{0.39}Al_{0.07}\}_{\Sigma 3.00}(O_{17.09}OH_{0.04}\square_{0.87})_{\Sigma 18.00}$

5c/10[2]: $\{(Nb_{0.25}Ta_{0.02}\square_{0.16})(Al_{0.22}Fe_{0.03}Ti_{0.01})\square_{0.31}\}_{\Sigma 1.00}Al_6B\{Si_{1.90}P_{0.03}(Sb_{0.52}As_{0.44}Al_{0.11})\}_{\Sigma 3.00}(O_{17.01}OH_{0.02}\square_{0.97})_{\Sigma 18.00}$

largely because of its higher As and lower Si contents compared to the holtite-group minerals.

Structural formulae for the three minerals are based on the endmembers in the classification developed by Pieczka *et al.* (2013), which are $(Nb_{0.6}\square_{0.4})Al_6B_3Si_3O_{18}$, $(Ti_{0.75}\square_{0.25})Al_6B_3Si_3O_{18}$, and $\square Al_6BAs_3^{3+}O_{15}$ for nioboholtite, titanoholtite and szklaryite respectively. Vacancies at the Al1 site result from the requirements of charge balance: $0.6Nb^{5+} + 0.4\square \rightarrow {}^{Al1}Al^{3+}$, $0.75Ti^{4+} + 0.25\square \rightarrow {}^{Al1}Al^{3+}$, and $3As^{3+} + {}^{Al1}\square \rightarrow 3Si^{4+} + {}^{Al1}Al^{3+}$. Szklaryite is most clearly distinguished from dumortierite- and holtite-group minerals on the basis of occupancy of the Si/As sites at which the sum of the trivalent constituents exceeds Si (Fig. 4*a*). Charge balance requires that vacancies exceed 0.5 p.f.u. at the Al1 site, even after deduction of vacancies associated with pentavalent and tetravalent cations in holtite-group components (Pieczka *et al.*, 2013).

In order to identify members of the holtite group, cations must first be grouped in terms of

TABLE 4. Representative compositions of titanoholtite.

	#29[1]	#30[1]	#31[1]	#32[1]	av.[1]	sd[1]	33/1a[2]	33/1[2]	33/3[2]	33/5[2]
Wt.%										
P_2O_5	0.02	0.02	0.00	0.00	0.01	0.01	0.07	0.00	0.00	0.00
Nb_2O_5	0.56	0.66	0.87	0.47	0.64	0.16	0.96	0.62	0.52	0.62
Ta_2O_5	1.43	1.20	0.89	0.76	1.07	0.36	2.05	1.41	2.33	0.75
SiO_2	21.61	21.93	21.89	22.25	21.92	0.23	20.99	21.97	21.38	22.35
TiO_2	3.94	3.92	4.30	4.17	4.08	0.24	3.32	4.12	4.04	4.34
B_2O_3	4.64	4.31	4.99	4.64	4.64	0.32	5.50	5.60	5.53	5.61
Al_2O_3	50.13	50.17	50.07	50.15	50.13	0.25	50.33	51.47	50.43	51.57
As_2O_3	2.28	2.26	2.17	2.19	2.22	0.08	2.92	2.88	2.98	2.85
Sb_2O_3	11.74	11.54	11.23	11.36	11.47	0.19	13.14	11.86	12.42	12.55
FeO	0.00	0.44	0.14	0.05	0.16	0.18	0.11	0.12	0.11	0.00
Total	96.34	96.44	96.55	96.04	96.34	0.34	99.39	100.06	99.76	99.64
Contents of ions on the basis of (O,OH) = 18–As–Sb p.f.u.										
P^{5+}	0.002	0.002	0.000	0.000	0.001	0.001	0.007	0.000	0.000	0.000
Nb^{5+}	0.027	0.032	0.042	0.023	0.031	0.008	0.046	0.029	0.025	0.029
Ta^{5+}	0.042	0.035	0.026	0.022	0.031	0.011	0.059	0.040	0.066	0.021
Si^{4+}	2.329	2.365	2.341	2.390	2.356	0.027	2.210	2.273	2.238	2.307
Ti^{4+}	0.319	0.318	0.346	0.337	0.330	0.017	0.263	0.320	0.318	0.337
B^{3+}	0.863	0.803	0.921	0.860	0.862	0.054	1.000	1.000	1.000	1.000
Al^{3+}	6.368	6.376	6.313	6.349	6.351	0.034	6.247	6.275	6.222	6.274
As^{3+}	0.150	0.148	0.141	0.143	0.145	0.006	0.187	0.181	0.190	0.179
Sb^{3+}	0.522	0.514	0.496	0.504	0.509	0.011	0.571	0.506	0.537	0.492
Fe^{2+}	0.000	0.039	0.013	0.005	0.014	0.016	0.010	0.011	0.011	0.000
O^{2-}	17.328	17.339	17.364	17.353	17.346	0.016	17.242	17.313	17.274	17.330

[1] analysis with direct WDS determination of B_2O_3, performed at Caltech (USA);
[2] analysis with B_2O_3 calculated on the basis of stoichiometry, performed at University of Warsaw (Poland);
av. – average; sd – standard deviation. H_2O content is assumed to be absent because $Ti > Fe^{2+}$.

Titanoholtite chemical formulae:

#29: $\{(Ti_{0.32}Nb_{0.03}Ta_{0.04}\square_{0.10})Al_{0.37}\square_{0.14}\}_{\Sigma 1.00}Al_6B_{0.86}\{Si_{2.33}(Sb_{0.52}As_{0.15})\}_{\Sigma 3.00}(O_{17.33}\square_{0.67})_{\Sigma 18.00}$
#30: $\{(Ti_{0.28}Nb_{0.03}Ta_{0.04}\square_{0.08})(Al_{0.38}Ti_{0.04}Fe_{0.04})\square_{0.12}\}_{\Sigma 1.00}Al_6B_{0.80}\{Si_{2.37}(Sb_{0.51}As_{0.15})\}_{\Sigma 3.03}(O_{17.34}\square_{0.66})_{\Sigma 18.00}$
#31: $\{(Ti_{0.34}Nb_{0.04}Ta_{0.03}\square_{0.12})(Al_{0.29}Ti_{0.01}Fe_{0.01})\square_{0.16}\}_{\Sigma 1.00}Al_6B_{0.92}\{Si_{2.34}(Sb_{0.50}As_{0.14}Al_{0.02})\}_{\Sigma 3.00}(O_{17.36}\square_{0.64})_{\Sigma 18.00}$
#32: $\{(Ti_{0.33}Nb_{0.02}Ta_{0.02}\square_{0.10})(Al_{0.35}Fe_{0.01}Ti_{0.01})\square_{0.16}\}_{\Sigma 1.00}Al_6B_{0.86}\{Si_{2.39}(Sb_{0.50}As_{0.14})\}_{\Sigma 3.04}(O_{17.35}\square_{0.65})_{\Sigma 18.00}$

average[1]: $\{(Ti_{0.32}Nb_{0.03}Ta_{0.03}\square_{0.10})(Al_{0.35}Ti_{0.01}Fe_{0.01})\square_{0.15}\}_{\Sigma 1.00}Al_6B_{0.86}\{Si_{2.36}(Sb_{0.51}As_{0.14})\}_{\Sigma 3.01}(O_{17.35}\square_{0.65})_{\Sigma 18.00}$

33/1a: $\{(Ti_{0.25}Nb_{0.05}Ta_{0.06}\square_{0.15})(Al_{0.22}Ti_{0.01}Fe_{0.01})\square_{0.25}\}_{\Sigma 1.00}Al_6B\{Si_{2.21}(Sb_{0.57}As_{0.19}Al_{0.03})\}_{\Sigma 3.00}(O_{17.24}\square_{0.76})_{\Sigma 18.00}$
33/1[2]: $\{(Ti_{0.31}Nb_{0.03}Ta_{0.04}\square_{0.14})(Al_{0.23}Ti_{0.01}Fe_{0.01})\square_{0.23}\}_{\Sigma 1.00}Al_6B\{Si_{2.27}(Sb_{0.51}As_{0.18}Al_{0.04})\}_{\Sigma 3.00}(O_{17.31}\square_{0.69})_{\Sigma 18.00}$
33/2[2]: $\{(Ti_{0.31}Nb_{0.02}Ta_{0.07}\square_{0.15})(Al_{0.19}Ti_{0.01}Fe_{0.01})\square_{0.24}\}_{\Sigma 1.00}Al_6B\{Si_{2.24}(Sb_{0.54}As_{0.19}Al_{0.03})\}_{\Sigma 3.00}(O_{17.27}\square_{0.73})_{\Sigma 18.00}$
33/5[2]: $\{(Ti_{0.34}Nb_{0.03}Ta_{0.02}\square_{0.14})Al_{0.25}\square_{0.22}\}_{\Sigma 1.00}Al_6B\{Si_{2.31}(Sb_{0.49}As_{0.18}Al_{0.02})\}_{\Sigma 3.00}(O_{17.33}\square_{0.67})_{\Sigma 18.00}$

components corresponding to the szklaryite and dumortierite groups, and these should be subtracted. Dumortierite-group endmembers include dumortierite ($AlAl_6BSi_3O_{18}$), hydroxydumortierite ($\square Al_6BSi_3O_{15}(OH)_3$), magnesiodumortierite ($MgAl_6BSi_3O_{17}OH$), $(Mg_{0.5}Ti_{0.5})Al_6BSi_3O_{18}$ and the respective Fe^{2+} analogues of the last two. The small amount of Fe in the analyses of this study is assumed to be Fe^{2+} (Pieczka *et al*., 2013). If Fe > Ti, then the Ti is assumed to be completely taken up in the dumortierite-group endmember $(Fe_{0.5}Ti_{0.5})Al_6BSi_3O_{18}$; otherwise, the excess Ti (= Ti – Fe) contributes to the titanoholtite endmember. Thus, the total amount of dumortierite-group endmembers using the Al1 site

content of Al + Fe^{2+} + Ti if Ti < Fe, then Al + $2Fe^{2+}$ is used, where $2Fe^{2+}$ is a proxy for $(Fe_{0.5}Ti_{0.5})Al_6BSi_3O_{18}$, assuming that the $Fe^{3+}Al_6BSi_3O_{18}$ content is negligible. Given the charge-balance mechanisms described above, the total content of holtite group endmembers is 5/3(Nb+Ta) if Ti < Fe^{2+} and 5/3(Nb+Ta) + 4/3 (Ti-Fe^{2+}) if Ti > Fe. The relative contents of dumortierite, szklaryite and holtite groups are shown for the compositions of this study in Fig. 4*a*. For those analyses in which the holtite group is dominant, the proportions of holtite, nioboholtite and titanoholtite are shown in Fig. 4*b*.

In accordance with the recommended nomenclature for the dumortierite supergroup (Pieczka *et al.*, 2013), nioboholtite and titanoholtite belong to the holtite group within the dumortierite supergroup, whereas szklaryite is currently the only known representative of a potential szklaryite group within the dumortierite supergroup. In addition, the endmember $\square Al_6BAs_3^{3+}O_{15}$ is a significant component of holtite from Virorco, Argentina (Galliski *et al.*, 2012). Like szklaryite, this holtite has $As^{3+} > Sb^{3+}$. An Sb^{3+} analogue of szklaryite has not yet been discovered, but most other compositions representing the holtite group-minerals show $Sb^{3+} > As^{3+}$ (Pryce, 1971; Voloshin *et al.*, 1977, 1987; Pieczka and Marszałek, 1996; Groat *et al.*, 2009; Pieczka *et al.*, 2011), and thus the component $\square Al_6BSb_3^{3+}O_{15}$ plays an important role in the dumortierite supergroup.

Titanoholtite does not have the highest Ti contents reported in dumortierite-supergroup minerals. In addition to magnesiodumortierite (Chopin *et al.*, 1995), dumortierite containing substantial Ti, i.e. 4.6 wt.% and 5.10–5.24 wt.% TiO_2, was reported from Rogaland, Norway (Huijsmans *et al.*, 1982) and Mozambique (D. Visser, personal communication with Grew, 2002), respectively. Although these dumortierites are low in MgO (0.19–0.30 wt.%) and FeO (0–0.30 wt.%), neither can be named titanoholtite, because the amount of the titanoholtite component is less than the sum of the dumortierite-group components, i.e. dumortierite + its Fe^{2+}-Ti analogue + its Mg-Ti analogue +

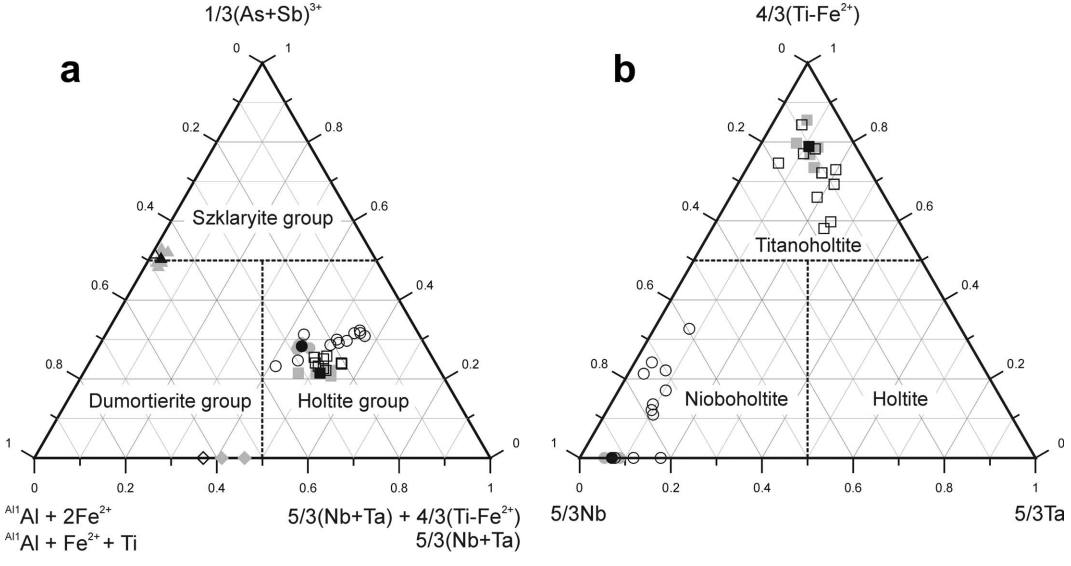

FIG. 4. Plot of nioboholtite, titanoholtite and szklaryite compositions on ternary diagrams that (*a*) differentiate dumortierite, holtite and szklaryite groups on the basis Al1 site occupants and Si/As site contents, and (*b*) distinguish members of the holtite group on the basis of Al1 content [see Pieczka *et al*. (2013) for details]. Note that the bottom corners of the left triangle have two alternative labels. The upper labels apply if total Ti > Fe; otherwise, the lower apply. Symbols: ▲, ● and ■ – spot analyses of type material of szklaryite, nioboholtite and titanoholtite performed at California Institute of Technology, Pasadena (USA); the same symbols in black – average compositions; open symbols – selected spot analyses performed at University of Warsaw (Poland); ◆ – titanian dumortierite (D. Visser, personal communication with Grew, 2002), ◇ – titanian dumortierite from Norway (Hujismans *et al*., 1982).

TABLE 5. Selected compositional data for the nioboholtite and titanoholtite co-type specimens.

	— Nioboholtite												– Titanoholtite			
	5b1	5b3	32/9	33/75	35/18	37a/13	37b/35	37c/9	38/15	42/77	8/5	34/54	37/10	40/8a	42/2	42/4
Wt.%																
P_2O_5	0.14	0.31	0.00	0.00	0.00	0.00	0.10	0.00	0.00	0.00	0.00	0.00	0.00	0.08	0.00	0.00
Nb_2O_5	4.37	5.16	5.30	4.82	4.98	4.59	4.68	5.28	3.91	5.26	1.05	0.79	0.97	0.60	0.77	1.37
Ta_2O_5	1.57	1.15	1.06	0.42	1.12	1.09	0.87	0.40	0.84	1.09	2.46	1.12	2.70	2.22	2.04	0.75
SiO_2	19.65	19.58	17.88	18.49	18.03	18.97	18.59	18.83	19.04	18.44	20.43	21.57	20.85	21.12	21.11	21.78
TiO_2	0.56	0.26	0.95	1.46	0.75	1.08	1.26	1.31	1.81	0.97	2.78	3.82	3.02	3.40	3.89	4.11
Al_2O_3	50.44	50.84	47.55	47.78	47.97	48.79	47.42	47.73	49.04	48.30	49.28	50.07	49.76	50.51	51.08	51.03
As_2O_3	3.90	4.39	2.14	2.17	2.26	2.11	2.42	2.17	2.45	2.55	2.72	2.88	2.75	2.85	2.58	2.50
Sb_2O_3	10.64	10.97	18.25	18.12	16.98	16.51	17.84	17.61	16.49	16.61	13.34	11.78	13.69	12.54	13.34	13.19
$B_2O_{3(calc.)}$	5.38	5.45	5.27	5.32	5.25	5.34	5.31	5.33	5.39	5.33	5.37	5.47	5.46	5.49	5.56	5.60
FeO	0.75	0.45	0.22	0.22	0.20	0.24	0.13	0.17	0.18	0.33	0.13	0.12	0.12	0.12	0.00	0.08
$H_2O_{(calc.)}$	0.03	0.03	0.00	0.00	0.00	0.00	0.00	0.00	0.00	0.00	0.00	0.00	0.00	0.00	0.00	0.00
Total	97.44	98.57	98.63	98.78	97.56	98.74	98.61	98.82	99.16	98.87	97.55	97.61	99.31	98.93	100.37	100.40
Contents of ions on the basis of (O,OH) = 18–As–Sb p.f.u.																
P^{5+}	0.013	0.028	0.000	0.000	0.000	0.000	0.009	0.000	0.000	0.000	0.000	0.000	0.000	0.007	0.000	0.000
Nb^{5+}	0.213	0.248	0.263	0.237	0.248	0.225	0.231	0.259	0.190	0.259	0.051	0.038	0.046	0.029	0.036	0.064
Ta^{5+}	0.046	0.033	0.032	0.012	0.034	0.032	0.026	0.012	0.025	0.032	0.072	0.032	0.078	0.064	0.058	0.021
Si^{4+}	2.116	2.082	1.964	2.013	1.990	2.057	2.029	2.046	2.048	2.006	2.203	2.286	2.212	2.229	2.200	2.253
Ti^{4+}	0.045	0.021	0.079	0.119	0.062	0.088	0.103	0.107	0.147	0.080	0.225	0.305	0.241	0.270	0.305	0.320
Al^{3+}	6.400	6.372	6.155	6.133	6.239	6.234	6.100	6.113	6.158	6.192	6.264	6.253	6.222	6.281	6.274	6.223
As^{3+}	0.255	0.283	0.143	0.143	0.151	0.139	0.160	0.143	0.160	0.168	0.178	0.185	0.177	0.183	0.163	0.157
Sb^{3+}	0.473	0.481	0.827	0.814	0.773	0.738	0.803	0.790	0.732	0.746	0.594	0.515	0.599	0.546	0.574	0.563
B^{3+}	1.000	1.000	1.000	1.000	1.000	1.000	1.000	1.000	1.000	1.000	1.000	1.000	1.000	1.000	1.000	1.000
Fe^{2+}	0.067	0.040	0.021	0.020	0.019	0.022	0.012	0.015	0.016	0.030	0.012	0.011	0.010	0.010	0.000	0.007
O^{2-}	17.250	17.216	17.030	17.042	17.075	17.122	17.037	17.067	17.108	17.086	17.228	17.299	17.223	17.271	17.263	17.280
OH^-	0.022	0.019	0.000	0.000	0.000	0.000	0.000	0.000	0.000	0.000	0.000	0.000	0.000	0.000	0.000	0.000

Nioboholtite formulae:

Sz5b/1: $\{(Nb_{0.21}Ta_{0.05}\square_{0.14})(Al_{0.26}Ti_{0.05}Fe_{0.07})\square_{0.23}\}_{\Sigma 1.00}Al_6B\{Si_{2.12}P_{0.01}(Sb_{0.47}As_{0.26}Al_{0.14})\}_{\Sigma 3.00}(O_{17.25}OH_{0.02}\square_{0.73})_{\Sigma 18.00}$

Sz5b/3: $\{(Nb_{0.25}Ta_{0.03}\square_{0.16})(Al_{0.25}Ti_{0.02}Fe_{0.04})\square_{0.25}\}_{\Sigma 1.00}Al_6B\{Si_{2.08}P_{0.03}(Sb_{0.48}As_{0.28}Al_{0.12})\}_{\Sigma 3.00}(O_{17.22}OH_{0.02}\square_{0.76})_{\Sigma 18.00}$

Sz32/9: $\{(Nb_{0.26}Ta_{0.03}Ti_{0.06}\square_{0.21})(Al_{0.09}Ti_{0.02}Fe_{0.02})\square_{0.31}\}_{\Sigma 1.00}Al_6B\{Si_{1.96}(Sb_{0.83}As_{0.14}Al_{0.07})\}_{\Sigma 3.00}(O_{17.03}\square_{0.97})_{\Sigma 18.00}$

Sz33/75: $\{(Nb_{0.24}Ta_{0.01}Ti_{0.10}\square_{0.19})(Al_{0.10}Ti_{0.02}Fe_{0.02})\square_{0.32}\}_{\Sigma 1.00}Al_6B\{Si_{2.01}(Sb_{0.81}As_{0.14}Al_{0.03})\}_{\Sigma 3.00}(O_{17.04}\square_{0.96})_{\Sigma 18.00}$

Sz35a/18: $\{(Nb_{0.25}Ta_{0.03}Ti_{0.04}\square_{0.18})(Al_{0.15}Ti_{0.02}Fe_{0.02})\square_{0.30}\}_{\Sigma 1.00}Al_6B\{Si_{1.99}(Sb_{0.77}As_{0.15}Al_{0.09})\}_{\Sigma 3.00}(O_{17.08}\square_{0.92})_{\Sigma 18.00}$

"hydroxydumortierite". Formulae for the two compositions that Visser (personal communication with Grew, 2002) reported from Mozambique are $\{(Al_{0.32}Ti_{0.06}Fe^{2+}_{0.03}Mg_{0.03}\square_{0.16})_{\Sigma=0.61}(Ti_{0.31}\square_{0.08})_{\Sigma=0.39}\}Al_6B[Si_{2.99}Al_{0.01})O_{17.55}(OH)_{0.45}$ and $\{(Al_{0.34}Ti_{0.03}Mg_{0.03}\square_{0.16})_{\Sigma=0.56}(Ti_{0.35}\square_{0.09})_{\Sigma=0.44}\}Al_6B[Si_{2.96}Al_{0.04})O_{17.56}(OH)_{0.44}$. The titanoholtite component is dominant in the Szklary pegmatite because the components $\square Al_6BAs^{3+}_3O_{15}$ and $\square Al_6BSb^{3+}_3O_{15}$ are present at the expense of dumortierite-group components, resulting in titanoholtite being more abundant than the dumortierite-group components.

Acknowledgements

The authors thank Diederik Visser for unpublished analyses of dumortierite and Nancy Price for performing preliminary EBSD analyses of szklaryite at the University of Maine. Members of the IMA CNMNC, Andrew Christy and an anonymous reviewer are thanked for their comments on the new-mineral proposals and an earlier version of this manuscript. ESG is supported by U.S. National Science Foundation grant EAR 0837980 to the University of Maine; AP is supported by AGH UST grant no 11.11.140.319; RJE and LAG by an NSERC Discovery grant to LAG; GRR by NSF grant EAR-0947956. SEM, EBSD, and EPMA analyses at Caltech were carried out at the GPS Division Analytical Facility, which is supported, in part, by NSF Grants EAR-0318518 and DMR-0080065.

References

Alexander, V.D., Griffen, D.T. and Martin, J.T. (1986) Crystal chemistry of some Fe- and Ti-poor dumortierites. *American Mineralogist*, **71**, 786–794.

Brady, J.B. and Cherniak, D.J. (2010) Diffusion in minerals: An overview of published experimental diffusion data. Pp. 899–920 in: *Diffusion in Minerals and Melts* (Y. Zhang and D.J. Cherniak, editors). Reviews in Mineralogy and Geochemistry, **72**. Mineralogical Society of America and Geochemical Society, Chantilly, Virginia, USA.

Chopin, C., Ferraris, G., Ivaldi, G., Schertl, H.-P., Schreyer, W., Compagnoni, R., Davidson, C. and Davis, A.M. (1995) Magnesiodumortierite, a new mineral from very-high-pressure rocks (western Alps). II. Crystal chemistry and petrological significance. *European Journal of Mineralogy*, **7**, 525–535.

Sz37a/13: $\{(Nb_{0.23}Ta_{0.03}Ti_{0.07}\square_{0.18})(Al_{0.17}Ti_{0.02}Fe_{0.02})\square_{0.28}\}_{\Sigma1.00}Al_6B\{Si_{2.06}(Sb_{0.74}As_{0.14}Al_{0.07})\}_{\Sigma3.00}(O_{17.12}\square_{0.88})_{\Sigma18.00}$

Sz37b/35: $\{(Nb_{0.23}Ta_{0.03}Ti_{0.09}\square_{0.20})(Al_{0.10}Ti_{0.01}Fe_{0.01})\square_{0.33}\}_{\Sigma1.00}Al_6B\{Si_{2.03}P_{0.01}(Sb_{0.80}As_{0.16})\}_{\Sigma3.00}(O_{17.04}\square_{0.96})_{\Sigma18.00}$

Sz37c/9: $\{(Nb_{0.26}Ta_{0.01}Ti_{0.09}\square_{0.20})(Al_{0.09}Ti_{0.02}Fe_{0.02})\square_{0.31}\}_{\Sigma1.00}Al_6B\{Si_{2.05}(Sb_{0.79}As_{0.14}Al_{0.02})\}_{\Sigma3.00}(O_{17.07}\square_{0.93})_{\Sigma18.00}$

Sz38/15: $\{(Nb_{0.19}Ta_{0.02}Ti_{0.13}\square_{0.17})(Al_{0.16}Ti_{0.02}Fe_{0.02})\square_{0.29}\}_{\Sigma1.00}Al_6B\{Si_{2.05}(Sb_{0.73}As_{0.16}Al_{0.06})\}_{\Sigma3.00}(O_{17.11}\square_{0.89})_{\Sigma18.00}$

Sz42/77: $\{(Nb_{0.26}Ta_{0.03}Ti_{0.05}\square_{0.20})(Al_{0.11}Ti_{0.03}Fe_{0.03})\square_{0.29}\}_{\Sigma1.00}Al_6B\{Si_{2.01}(Sb_{0.75}As_{0.16}Al_{0.08})\}_{\Sigma3.00}(O_{17.09}\square_{0.91})_{\Sigma18.00}$

Titanoholtite formulae:

Sz8/5: $\{(Ti_{0.22}Nb_{0.05}Ta_{0.07}\square_{0.15})(Al_{0.24}Ti_{0.01}Fe_{0.01})\square_{0.25}\}_{\Sigma1.00}Al_6B\{Si_{2.20}(Sb_{0.59}As_{0.18}Al_{0.03})\}_{\Sigma3.00}(O_{17.23}\square_{0.77})_{\Sigma18.00}$

Sz34/54: $\{(Ti_{0.30}Nb_{0.04}Ta_{0.03}\square_{0.14})(Al_{0.24}Ti_{0.01}Fe_{0.01})\square_{0.23}\}_{\Sigma1.00}Al_6B\{Si_{2.29}(Sb_{0.51}As_{0.19}Al_{0.01})\}_{\Sigma3.00}(O_{17.30}\square_{0.70})_{\Sigma18.00}$

Sz37/10: $\{(Ti_{0.23}Nb_{0.05}Ta_{0.08}\square_{0.16})(Al_{0.21}Ti_{0.01}Fe_{0.01})\square_{0.26}\}_{\Sigma1.00}Al_6B\{Si_{2.21}(Sb_{0.60}As_{0.18}Al_{0.01})\}_{\Sigma3.00}(O_{17.22}\square_{0.78})_{\Sigma18.00}$

Sz40/8a: $\{(Ti_{0.26}Nb_{0.03}Ta_{0.06}\square_{0.15})(Al_{0.25}Ti_{0.01}Fe_{0.01})\square_{0.23}\}_{\Sigma1.00}Al_6B\{Si_{2.23}P_{0.01}(Sb_{0.55}As_{0.18}Al_{0.03})\}_{\Sigma3.00}(O_{17.27}\square_{0.73})_{\Sigma18.00}$

Sz42/2: $\{(Ti_{0.30}Nb_{0.04}Ta_{0.06}\square_{0.15})Al_{0.21}\square_{0.24}\}_{\Sigma1.00}Al_6B\{Si_{2.20}(Sb_{0.57}As_{0.17}Al_{0.06})\}_{\Sigma3.00}(O_{17.26}\square_{0.74})_{\Sigma18.00}$

Sz42/4: $\{(Ti_{0.31}Nb_{0.06}Ta_{0.02}\square_{0.15})(Al_{0.20}Ti_{0.01}Fe_{0.01})\square_{0.24}\}_{\Sigma1.00}Al_6B\{Si_{2.25}(Sb_{0.56}As_{0.16}Al_{0.03})\}_{\Sigma3.00}(O_{17.28}\square_{0.72})_{\Sigma18.00}$

Fuchs, Y., Ertl, A., Hughes, J.M., Prowatke, S., Brandstaetter, F. and Schuster, R. (2005) Dumortierite from the Gföhl unit: Lower Austria; chemistry, structure, and infra-red spectroscopy. *European Journal of Mineralogy*, **17**, 173–183.

Galliski, M.A., Márques-Zavalía, M.F., Lira, R., Cempírek, J. and Škoda, R. (2012) Mineralogy and origin of the dumortierite-bearing pegmatites of Virorco, San Luis, Argentina. *The Canadian Mineralogist*, **50**, 873–894.

Grew, E.S. (2002) Borosilicates (exclusive of tourmaline) and boron in rock-forming minerals in metamorphic environments. Pp. 387–502 in: *Boron: Mineralogy, Petrology, and Geochemistry* (L.M. Anovitz and E.S. Grew, editors). Reviews in Mineralogy, **33**, Mineralogical Society of America, Washington, D.C.

Grew, E.S., Graetsch, H., Pöter, B., Yates, M.G., Buick, I., Bernhardt, H.-J., Schreyer, W., Werding, G., Carson, C.J. and Clarke, G.L. (2008) Boralsilite, $Al_{16}B_6Si_2O_{37}$, and "boron-mullite": compositional variations and associated phases in experiment and nature. *American Mineralogist*, **93**, 283–299.

Groat, L.A., Grew, E. S., Evans, R.J., Pieczka, A. and Ercit, T.S. (2009) The crystal chemistry of holtite. *Mineralogical Magazine*, **73**, 1033–1050.

Hoskins, B.F., Mumme, W.G. and Pryce, M.W. (1989) Holtite, $(Si_{2.25}Sb_{0.75})B[(Al_6(Al_{0.43}Ta_{0.27}\square_{0.30})O_{15}(O,OH)_{2.25}]$: crystal structure and crystal chemistry. *Mineralogical Magazine*, **53**, 457–463.

Huijsmans, J.P.P., Barton, M. and van Bergen, M.J. (1982) A pegmatite containing Fe-rich grandidierite, Ti-rich dumortierite and tourmaline from the Precambrian, high-grade metamorphic complex of Rogaland, S.W. Norway. *Neues Jahrbuch für Mineralogie Abhandlungen*, **143**, 249–261.

Ma, C. and Rossman, G.R. (2008) Barioperovskite, $BaTiO_3$, a new mineral from the Benitoite Mine, California. *American Mineralogist*, **93**, 154–157.

Ma, C. and Rossman, G.R. (2009) Tistarite, Ti_2O_3, a new refractory mineral from the Allende meteorite. *American Mineralogist*, **94**, 841–844.

Ma, C., Goreva, J.S. and Rossman, G.R. (2002) Fibrous nanoinclusions in massive rose quartz: HRTEM and AEM investigations. *American Mineralogist*, **87**, 269–276.

Moore, P.B. and Araki, T. (1978) Dumortierite, $Si_3B[Al_{6.75}\square_{0.25}O_{17.25}(OH)_{0.75}]$: a detailed structure analysis. *Neues Jahrbuch für Mineralogie Abhandlungen*, **132**, 231–241.

Pieczka, A. (2000) A rare mineral-bearing pegmatite from the Szklary serpentinite massif, the Fore-Sudetic Block, SW Poland. *Geologia Sudetica*, **33**, 23–31.

Pieczka, A. (2007) Blue dravite from the Szklary pegmatite (Lower Silesia, Poland). *Mineralogia Polonica*, **38/2**, 209–218.

Pieczka, A. (2010) Primary Nb-Ta minerals in the Szklary pegmatite, Poland: new insights into controls of crystal chemistry and crystallization sequences. *American Mineralogist*, **95**, 1478–1492.

Pieczka, A. and Kraczka, J. (1996) X-ray and Mössbauer study of black tourmalines (schorls) from Szklary (Lower Silesia, Poland). *Mineralogia Polonica*, **27/2**, 33–40.

Pieczka, A. and Marszałek, M. (1996) Holtite – the first occurrence in Poland. *Mineralogia Polonica*, **27**, 3–8.

Pieczka, A., Grew, E. S., Groat, L.A. and Evans, R.J. (2011) Holtite and dumortierite from the Szklary Pegmatite, Lower Silesia, Poland. *Mineralogical Magazine*, **75**, 303–315.

Pieczka, A., Evans, R.J., Grew, E.S., Groat, L.A., Ma, C. and Rossman, G.R. (2013) The dumortierite supergroup. I. A new nomenclature for the dumortierite and holtite groups. *Mineralogical Magazine*, **77**, 2825–2839.

Pouchou, J.L. and Pichor, F. (1985) "PAP" (phi-rho-z) procedure for improved quantitative microanalysis. Pp. 104–106 in: *Microbeam Analysis* (J.T. Armstrong, editor). San Francisco Press, San Francisco, California, USA.

Pryce, M.W. (1971) Holtite: a new mineral allied to dumortierite. *Mineralogical Magazine*, **38**, 21–25.

Sorbier, L., Rosenberg, E. and Merlet, C. (2004) Microanalysis of porous materials. *Microscopy and Microanalysis*, **10**, 745–752.

Timmermann, H., Parrish, R.R., Noble, S.R. and Kryza, R. (2000) New U-Pb monazite and zircon data from the Sudetes Mountains in SW Poland; evidence for a single-cycle Variscan Orogeny. *Journal of the Geological Society*, **157**, 265–268.

van Breemen, O., Bowes, D.R., Aftalion, M. and Żelaźniewicz, A. (1988) Devonian tectonothermal activity in the Sowie Góry gneissic block, Sudetes, southwestern Poland: evidence from Rb-Sr and U-Pb isotopic studies. *Journal of the Polish Geological Society*, **58**, 3–10.

Voloshin, A.V., Gordienko, V.V., Gel'man, Ye.M., Zorina, M.L., Yelina, N.A., Kul'chitskaya, Ye.A., Men'shikov, Yu.P., Polezhayeva, L.I., Ryzhova, R.I., Sokolov, P.B. and Utochkina, G.I. (1977) Holtite (first find in the USSR) and its relationship with other tantalum minerals in rare-metal pegmatites. *Zapiski Vsesoyuznogo Mineralogicheskogo Obshchestva*, **106**(3), 337–347 (in Russian).

Voloshin, A.V., Pakhomovskiy, Ya.A. and Zalkind, O.A. (1987) An investigation of the chemical composition and IR-spectroscopy of holtite. Pp. 14–34 in: *Mineral'nyye Assotsiatsii i Mineraly Magmaticheskikh Kompleksov Kol'skogo Poluostrova*. Kol'skiy Filial Akademii Nauk SSSR, Apatity (in Russian).